

SYNTHESIS AND PHYSICOCHEMICAL CHARACTERISATION OF (Si,Ga)-MCM-22 ZEOLITE. TOLUENE DISPROPORTIONATION REACTION

I. Fechete^{1,2*}, E. Dumitriu¹, P. Caullet², D. Lutic³, H. Kessler²

¹*Laboratory of Catalysis, "Gh. Asachi" Technical University of Iasi,
71 D. Mangeron Av., 700050, Iasi, Romania*

²*Laboratoire de Matériaux à Porosité Contrôlée, UPRES-A 7016,
ENSCMu-UHA, 3 rue A. Werner, 68093 Mulhouse, France*

³*Faculty of Chemistry, "Al. I. Cuza" University of Iasi,
11, Bd. Carol I, Iasi, Romania*

*Corresponding author: Ioana.Fechete@ecpm.u-strasbg.fr

Received: 12/11/2007

Accepted after revision: 03/12/2007

Abstract: Three samples of (Si,Ga)-MCM-22 zeolites (IZA code MWW) with Si/Ga ratios of 18, 71 and 89 were synthesized hydrothermally under static conditions, using hexamethyleneimine as a structural directing agent (SDA). The pure phase of zeolite was obtained only for Si/Ga = 18, while for the other ratios one unknown phase was detected. SEM, XRD, TG-ATD, BET, ⁷¹Ga and ²⁹Si NMR MAS spectroscopies were performed, confirming the isomorphous substitution of gallium into the zeolite structure. The acidic properties were studied by TPD of ammonia, showing that the acid character depends on the gallium concentration. The catalytic performances of (Si,Ga)-MCM-22 zeolite with various Ga contents were studied in the toluene disproportionation reaction in the temperature range 573-673 K. We showed that the fraction of *p*-xylene increases with the isomorphous substitution degree and decreases with the temperature and also that the catalytic performances are correlated with the structure and the acidic properties of the (Si,Ga)-MCM-22 zeolite.

Key words: *isomorphous substitution; (Si,Ga)-MCM-22 zeolite; p-xylene*

INTRODUCTION

Among the reactions of aromatic hydrocarbons conversion, the toluene disproportionation reaction has been intensively studied, and it can be regarded as the first process applied on an industrial scale for the utilization of the toluene surplus, in order to produce benzene and xylenes. Especially *p*-xylene is the most valuable xylene isomer due to its importance for the production of the polyester fibers via terephthalic acid and for the manufacture of poly-(ethylene terephthalate) for recyclable bottles and benign environment [1, 2]. The success in the formation of *p*-xylene is due to the catalyst type, its acidity and the reaction conditions.

Various zeolites have been used as catalyst in toluene disproportionation [3 – 9], but the fraction in *p*-xylene isomers was close to the equilibrium value (~ 24 %). It is very well known that the disproportionation of toluene involves a bulky intermediate occurrence of a bimolecular reaction mechanism [4, 10], thus the MCM-22 zeolite which combines the catalytic properties of zeolite with 10-MR and 12-MR is very promising for these reactions. The Al-MCM-22 [11], dealuminated Al-MCM-22 [12] and MCM-22 zeolite modified with indium [13], have been tested in toluene disproportionation reaction and it has been shown that the complex structure and the acidity of the sample plays a significant role in the selective formation of *p*-xylene.

MCM-22 [14] is a member of the MWW family of zeolites. The zeolite is composed of interconnected $\{4^35^66^3[4^3]\}$ building units that form a three-dimensional dodecasil-1H-like lattice belonging to the *P6/mmm* space group [15]. Its particular structure contains two independent noninterconnected pore systems accessible through 10-MR openings [15] and 12-MR on the external surface [16, 17]. One of the pore system, tridimensional, is composed of supercages (inner diameter of 7.1 Å and height of 18.4 Å) interconnected by channels of 4.0 x 5.5 Å. The other consists of two dimensional sinusoidal channels of 4.1 x 5.1 Å [18]. A constraint index (CI) of 1.8 (characteristic of a 12-MR) [19] and 4.6 (characteristic of a 10-MR) [20] and a spaciousness index of 8, places the zeolite MCM-22 between 10- and 12-MR zeolites [21].

Generally, the zeolites have three types of acidic sites namely weak, medium and strong. The strong acid sites are responsible for the undesired reactions. Therefore, it is necessary to modify the acidity of these zeolites in order to achieve the selectivity for a typical reaction. One way of accomplishing this is the isomorphous replacement of Al by other trivalent ions, like Ga. Moreover, it is known that the isomorphous substitution in the zeolite framework by heteroatoms produces new materials with significantly modified physicochemical and catalytic properties [22].

In this work, we report the synthesis of (Si,Ga)-MCM-22 zeolite with different Si/Ga ratios, obtained under static conditions at 423 K and the physicochemical characterization of these samples. To our knowledge, the studies on the synthesis of isomorphously substituted (Si,Ga)-MCM-22 zeolite have not been enough reported. Kumar et al [23] have reported the Ga/MCM-22, but prepared by ion exchanged MCM-22. Also, we report the catalytic performances of the (Si,Ga)-MCM-22 zeolite in toluene disproportionation reaction.

EXPERIMENTAL

Catalysts synthesis

The samples of (Si,Ga)-MCM-22 zeolite have been synthesized by hydrothermal crystallisation technique, using the following reagents: Aerosil 200 (Degussa, 99.8% SiO₂), Sodium Hydroxide (Prolabo, NaOH 98%), Hexamethyleneimine (Aldrich, HMI, C₆H₁₃N > 99%) and Amorphous Gallium Oxide - GaOOH (H₂O)_{0.5} (prepared by evaporation of gallium nitrate solution, Ga(NO₃)₃, Rhone-Poulenc). Deionized water was used throughout, for the gel preparation and for the washing of the final products. We have used the following synthesis procedure: the sodium hydroxide was dissolved in $\frac{3}{4}$ the necessary water. The silica source - Aerosil 200 was added to this solution subsequently under vigorous stirring. After all silica was incorporated, the gallium source was added - the suspension of GaOOH dissolved in $\frac{1}{4}$ of water. The resulting gel was heated at 333 K for 12 h with stirring, then cooled to about 298 K and the hexamethyleneimine was added dropwise. The final reaction mixture was then maintained for 6 h at 298 K with stirring. The molar chemical compositions of the mixture reactions are presented in Table 1.

The crystallization of the gels was carried out in stainless steel autoclaves without agitation at 423 K for 9 days. After the autoclaves had been cooled to the room temperature, the product was filtered, washed with deionized water, and dried at 353 K overnight to obtain the precursor of MCM-22 zeolite, noted as MCM-22 (P). In order to remove the template molecules from channels of zeolites, the samples of MCM-22 (P) zeolite were calcined at 803 K for 8 h in air. Then, the calcined samples were ion-exchanged with 1M NH₄NO₃ aqueous solution (liquid to solid ratio of 20 mL.g⁻¹) under continuous stirring at 353 K for 8 h, in order to convert the zeolite into ammonium forms (NH₄-(Si,Ga)-MCM-22). This procedure was repeated twice. After that, the ammonium form of zeolites was again calcined in air at 803 K for 4 h, in order to convert the zeolites to its acidic form, H-(Si,Ga)-MCM-22.

Catalysts characterization

The morphology of the samples was determined by scanning electron microscopy using a Philips XL 30 scanning electron microscope (SEM). The elemental analysis of the solids was performed by the Service Central d'Analyse of CNRS-Vernaison. The structure and the purity of the zeolite samples were determined by X-ray diffraction (STOE STADI P diffractometer - CuK α , λ = 1.5406 Å). The thermal analysis of the as-synthesized samples was performed on a SETARAM LABSYS. The experiments were carried out in nitrogen in the temperature range 298 – 1273 K with a heating rate of 5 K.min⁻¹. The BET surface areas were evaluated by means of the t-plot method, from nitrogen adsorption/desorption isotherm performed at 77 K with a MICROMERITICS ASAP 2100 system. The ⁷¹Ga MAS NMR spectra were recorded on a Bruker DSX-400 spectrometer and the single-pulse technique was used under the following conditions: chemical shift standard: Ga(NO₃)₃; pulse length = 0.7 μ s; pulse angle = $\pi/12$; recycle time: 0.5 s; spinning rate = 10 KHz; number of scans = 10 000. The ²⁹Si MAS NMR spectra were recorded on Bruker MSL-300 spectrometer under the following conditions: chemical shift standard: TMS; frequency = 59.63 MHz; pulse length = 5 μ s;

pulse angle = $\pi/2$; recycle time 100 s; spinning rate = 4 KHz; number of scans = 290. The acidity of the samples was measured by temperature programmed desorption (TPD) using ammonia as probe. Prior to TPD experiments, the solids were pre-treated in an air flow at 823 K for 1 h. Ammonia was adsorbed for 15 min at 383 K. The physisorbed ammonia was removed by evacuation of the sample at 383 K for 1 h, in a dry helium stream. The ammonia desorption was carried out in helium stream at a heating rate of 10 K.min⁻¹ up to 823 K. The amount of desorbed ammonia was monitored with a conductivity cell. The total amount of desorbed NH₃ was determined by back titration with NaOH in N/10 HCl.

Catalytic tests

The toluene disproportionation was carried out in a pulse-type microreactor coupled with GC. The microreactor consisted of a stainless steel tube (o.d. 6 mm, i.d. 3.5 mm, and length 90 mm) containing 40 mg of catalyst (without binder) with particle size 0.25-0.5 mm packed between two quartz wool plugs. This allowed us obtain a ca. 3.5 mm x 5 mm cylindrical fixed bed of catalyst, which was found to be optimal for avoiding diffusion-controlled phenomena. Before reaction, the catalyst was activated or regenerated in air stream at 773 K for 2.5 h, followed by cooling to the temperature of the reaction in a nitrogen flow. Samples of 0.1 μ L of reagents were injected at constant temperature. Nitrogen was used as a carrier gas (30 mL.min⁻¹ flow rate). The reaction products were analyzed on line by GC, using a 4.5 m column packed with 16 % SE-30 + 3 % Benton 34 on Chromosorb W-AWDCMS and a FI detector.

RESULTS AND DISCUSSION

Synthesis

The molar chemical compositions of the reaction mixtures for the three samples of (Si,Ga)-MCM-22 zeolite and the synthesis conditions are given in the Table 1. The results of the synthesis are also given in Table 1. The pure phase of (Si,Ga)-MCM-22 zeolite and well-crystallized product under static conditions was obtained only for Si/Ga = 18. For other Si/Ga ratios, the crystallization of the MCM-22 zeolite also occurred but an unknown phase is detected.

Table 1. The molar chemical composition of the reaction mixture, synthesis conditions and the results of the synthesis of (Si,Ga)-MCM-22 zeolite; 9 days; $T = 423$ K

Sample	Molar chemical composition of the reaction mixture				Phase (XRD)
	SiO ₂ /Ga ₂ O ₃	Na ₂ O/SiO ₂	HMI/SiO ₂	H ₂ O/SiO ₂	
A	30	0.16	0.50	45	MCM-22 (P)
B	150	0.19	0.52	44	MCM-22 (P) + un.
C	200	0.21	0.52	44	MCM-22 (P) + un.

un.: unidentified phase (d values = 18.1 Å)

Characterisation

The results of the elemental analysis are given in Table 2. By comparing the composition of the gels and the as-synthesized samples, we can conclude that all gallium was incorporated into the product, indicating that the present synthesis method is effective for Ga incorporation. For the calcined samples, the Si/Ga ratio was higher than that of the as-synthesized samples. These results indicate that only part of the gallium present in the gels is present into the framework, indicating the degallation by calcination, particularly for the sample A.

Table 2. The physicochemical characteristics of (Si,Ga)-MCM-22 zeolite

Sample	Si/Ga			V [Å ³] ^c	Surface area [m ² .g ⁻¹]	Micropore volume [cm ³ .g ⁻¹]	Weight loss [%] 298 – 1273 K
	gel	precursor ^a [2D]	calcined ^b [3D]				
A	15	16	18	4432	521	0.18	24.5
B	75	64	71	4376	454	0.18	20.4
C	100	82	89	4351	427	0.17	18.7

a,b: determined from elemental analysis

c: calculated from the XRD of the calcined samples

The morphology of the samples A and C of the (Si,Ga)-MCM-22 zeolite obtained under static synthesis conditions at 423 K is shown in the SEM images in Figure 1. It is similar to that reported for the (Si,Al)-MCM-22 zeolite samples [24, 25]. Gallium incorporation seems not to induce changes in the morphology of the MCM-22 crystals zeolite. The crystals have hexagonal platelet morphology. The sample B of (Si,Ga)-MCM-22 zeolite (not shown) have a similar crystal morphology.

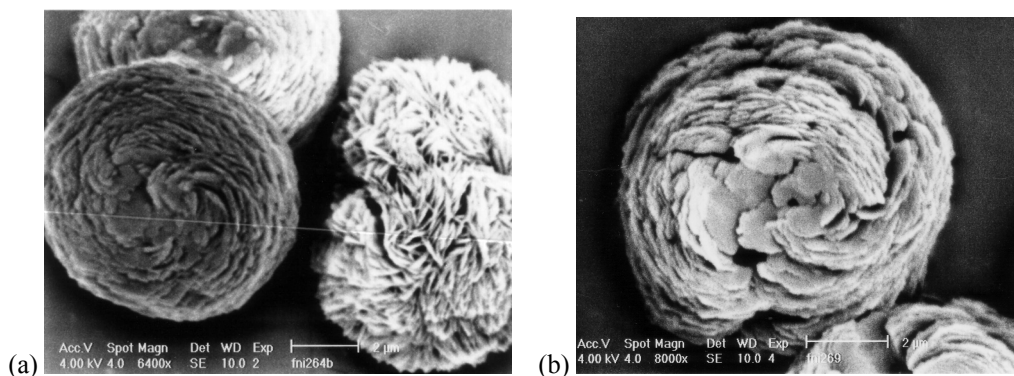


Figure 1. Scanning electron micrographs of samples A (a) and C (b) of (Si,Ga)-MCM-22 zeolite

In Figures 2 – 3, typical XRD patterns of precursor (Si,Ga)-MCM-22 (P) (2D) and calcined (Si,Ga)-MCM-22 (3D) sample A are presented. They are very similar to that of its aluminosilicate analogues reported [24, 26, 27]. For the sample A, no impurities were detected. For the samples B and C (not shown), the unknown phase is formed together with the MCM-22 phase. This unidentified phase is characterized by a diffraction peak at $2\theta = 4.88$ (d-spacing of 18.1 Å) in the calcined samples.

The values of the unit cell volume (\AA^3) for the calcined samples of (Si,Ga)-MCM-22 zeolite with different ratios increase with the incorporation of gallium into the framework (Table 2). The expansion ($\sim 1.86\%$) in the unit cell volume calculated between the samples A and C is due to the incorporation of gallium into the framework.

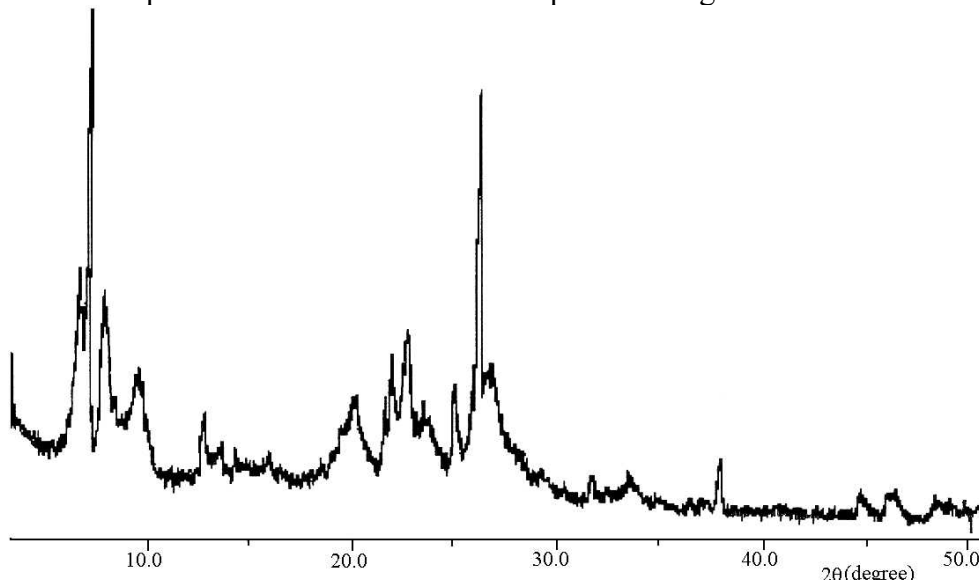


Figure 2. X-ray powder diffraction pattern of the as-synthesized sample A of (Si,Ga)-MCM-22 zeolite

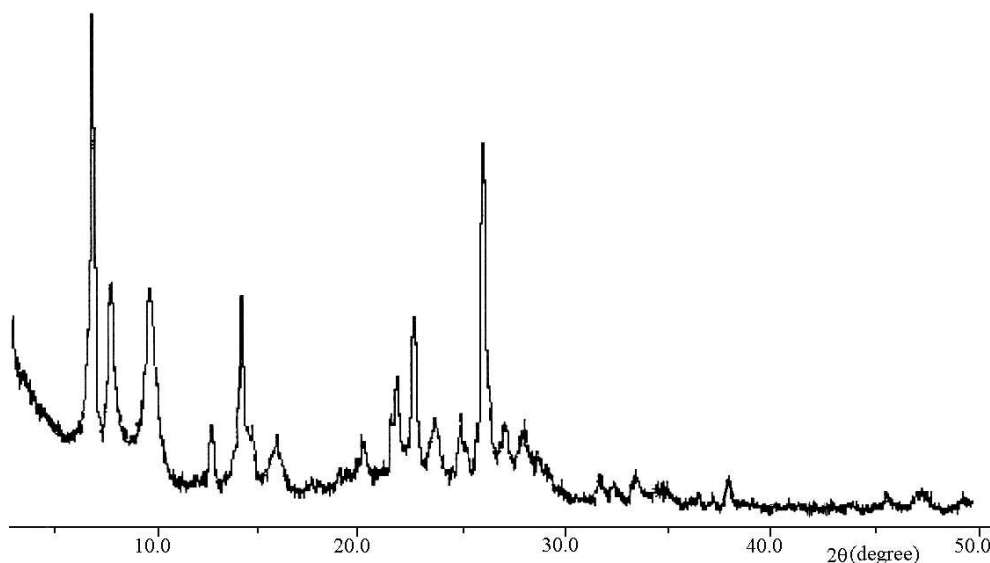


Figure 3. X-ray powder diffraction pattern of the calcined sample A of (Si,Ga)-MCM-22 zeolite

The total BET surface areas detected of the calcinated samples was beetwen 427 – 521 $\text{m}^2\cdot\text{g}^{-1}$ (Table 2). The BET surface area is much greater for the sample A of (Si,Ga)-MCM-22 zeolite indicating a high cristallinity of the sample, and is reduced with the decrease in galium content. The difference in the values of the samples B and C, is probably due to the presence of the amorph/impurities phases. The micropores volume

measured of samples A and B ($0.18 \text{ cm}^3 \cdot \text{g}^{-1}$) is also more than for the sample C ($0.17 \text{ cm}^3 \cdot \text{g}^{-1}$). The results for BET surface areas and the micropore volume are comparable with those reported in the literature for (Si,Al)-MCM-22 zeolite [28 – 31].

Thermogravimetric experiments of the (Si,Ga)-MCM-22 zeolite showed the same general behavior as its aluminosilicates analogues [24, 26]. The weight loss up to 473 K is due to the water desorption, and between 473 K and 1273 K is due to the decomposition of organic template, hexamethyleneimine, respectively. Weight losses of 24.5 for the sample A may be due to a higher gallium content and/or to better crystallinity compared with the samples B and C (Table 2).

The ^{71}Ga MAS NMR spectra for the as-synthesized sample A of (Si,Ga)-MCM-22 is presented in Figure 4a. Contrary to its analogue (Si,Al)-MCM-22 zeolite, which shows two peaks assigned to the four coordinated framework aluminium [26, 31, 32], the precursor sample of (Si,Ga)-MCM-22 zeolite shows one single signal located at 151 ppm, indicating the presence of the Ga in the tetrahedral framework. For the calcinated sample A (Figure 4b), two signals are detected at 135 and -8 ppm, assigned to the Ga in the tetrahedral framework and to the octahedral Ga species into extraframework. It can be seen that the calcination leads to the formation of the extraframework Ga species. These results are in good agreement with those reported in the literature for the other structures containing gallium [33 – 36].

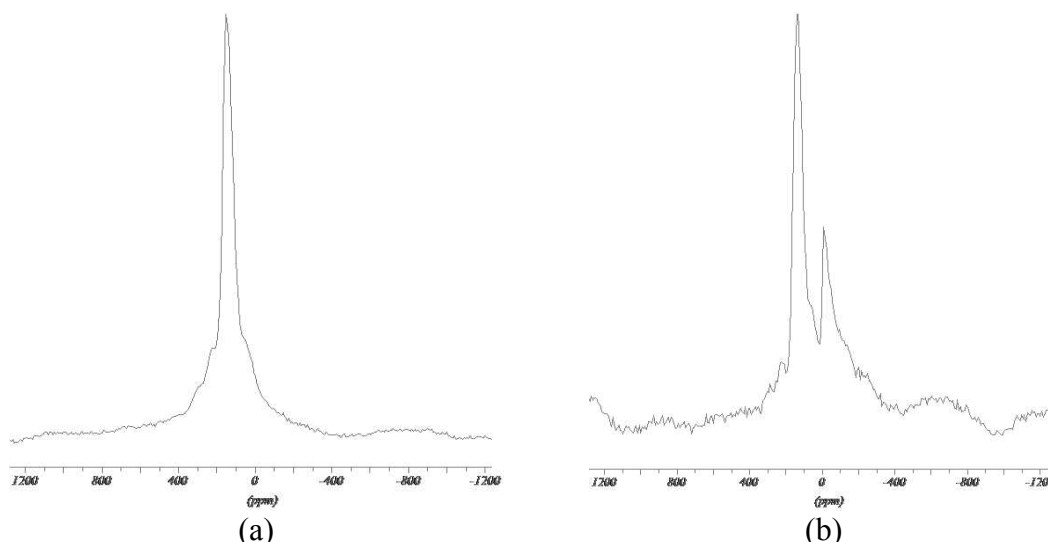


Figure 4. ^{71}Ga MAS NMR spectra of the precursor (a) and calcined (b) sample A of (Si,Ga)-MCM-22 zeolite

The ^{29}Si MAS NMR spectrum for the precursor sample A of (Si,Ga)-MCM-22 zeolite (Figure 5a) shows seven peaks at chemical shifts of -117.58, -116.21, -113.34, -109.98, -103.40, -97.99, and -90.24 ppm. In the calcined sample, the ^{29}Si MAS NMR spectrum (Figure 5b) presented five peaks well resolved at: -117.77, -112.51, -110.85, -104.57 and -98.43 ppm, shifted mainly to high field strength with one exception for the low field strength. The disappearance (or slow resolved) of the two peaks can be observed around -90.24 and -116.21 ppm. After calcination the peak intensity decreases and this fact can be due to the degallation from the framework as confirmed in the ^{71}Ga MAS NMR.

Camlor et al. [27] have reported the existence of the seven peaks very well resolved on the ITQ pure silica, analog of MCM-22, while Hunger et al. [37] have reported five peaks on the (Si,Al)-MCM-22 zeolite. The five peaks can be due to the wide distribution of T-O-T bonds ranging from 138 to 164 [38]. By comparing the values of the chemical shifts reported in the literature for ITQ pure silica, analog of MCM-22 and (Si,Al)-MCM-22 zeolite [27, 37, 39, 40], with those reported for (Si,Ga)-MCM-22 zeolite, the signal at -90 ppm is assigned to $\text{Si}(\text{OSi})_2(\text{OH})_2$, the signal at ~ -98 ppm is due to $\text{Si}(\text{1Ga 3Si})$ and $\text{Si}(\text{OSi})_3 \text{ OH}$ defect, while the others between ~ -117 and -103 ppm correspond to $\text{Si}(\text{0Ga})$ sites.

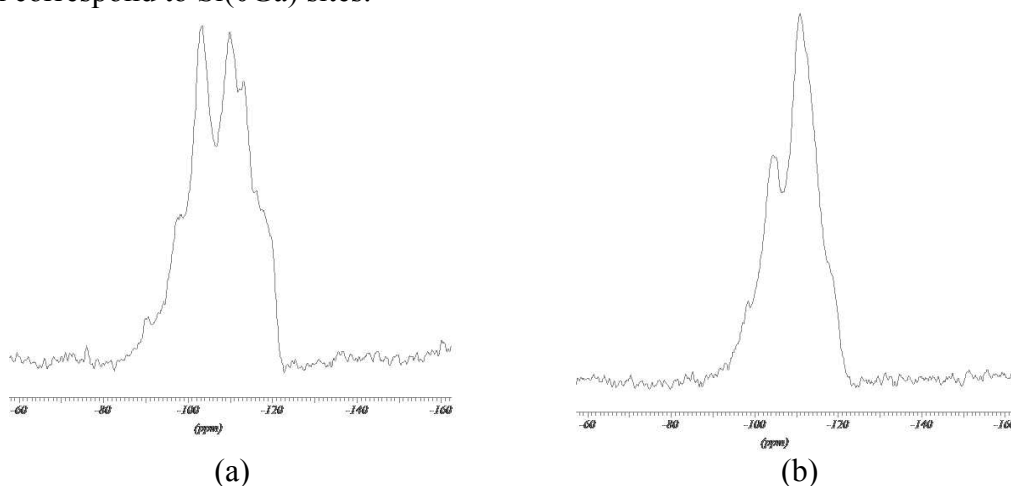


Figure 5. ^{29}Si MAS NMR spectra of the precursor (a) and calcined (b) sample A of (Si,Ga)-MCM-22 zeolite

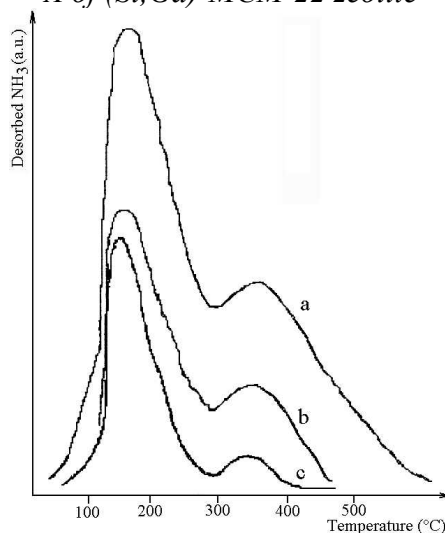


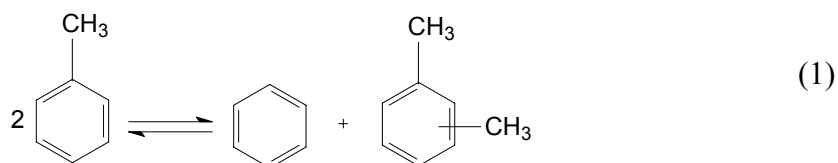
Figure 6. NH_3 -TPD profiles of the sample A (a), B (b) and C (c) of (Si,Ga)-MCM-22 zeolite

The TPD curves for the three samples of H-form (Si,Ga)-MCM-22 zeolite are given in Figure 6 and the corresponding acidity values in $\text{mmol NH}_3 \cdot \text{g}^{-1}$ are the following: 2.9 (sample A), 2.1 (sample B) and 1.5 (sample C). Two desorption peaks clearly appeared, respectively, at 423 – 448 K and in the temperature range of 623 – 648 K. The first peak is attributed to physisorbed NH_3 and was related to weak Lewis acid sites [21], while the

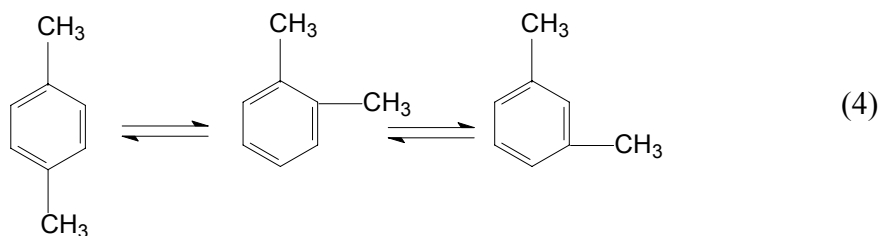
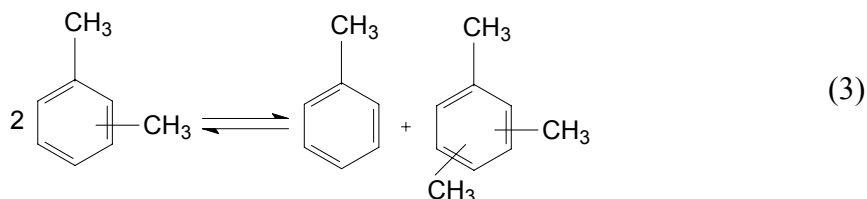
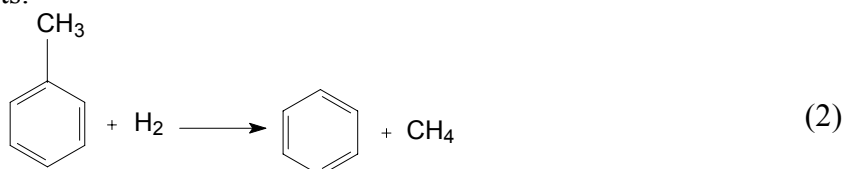
second peak corresponds to the decomposition of NH_4^+ ions and is generally attributed to Bronsted sites [21, 41], which could be associated with Lewis sites [32]. The TPD data owing to the three samples of the (Si,Ga)-MCM-22 zeolite have been associated with the weak and medium acid sites.

Toluene disproportionation

The disproportionation of toluene is one of the important petrochemical processes used to produce *p*-xylene [42], the most important and desired among the xylene isomers. Continuous efforts are made in order to improve its composition beyond the thermodynamic value (~ 24 %). The performance of (Si,Ga)-MCM-22 zeolite with Si/Ga ratio different for toluene disproportionation will be presented further. Concerning the disproportionation equation, two toluene molecules give xylene isomers and benzene as primary products (eq.1).



The disproportionation reaction may be accompanied by secondary reactions like dealkylation reaction of toluene to benzene (eq. 2), and also by a xylenes disproportionation (versus toluene and trimethylbenzenes) (eq. 3) and isomerisation reactions of xylenes (eq. 4). Only traces of trimethylbenzenes and ethylbenzene were produced as by-products.



It is well known that the variation of the temperature would induce variation in catalytic activity and isomorphous substitution phenomenon can modify the acidity strength of the catalysts and implicit the catalytic activity [22, 43 – 45]. In this sens, the effect of the reaction temperature and isomorphous degree on the total conversion of toluene

were examined over the three samples of (Si,Ga)-MCM-22 with different Si/Ga ratios in the temperature range 573 – 673 K. It can be observed in Figure 7 that the total toluene conversion increases with the increase in reaction temperature for all the samples. Also, it can be seen that for all the temperatures studied, the catalytic activity is highest for the sample A, which is the most acidic sample (in fact the acid sites of Bronsted forts are implied in the reaction of dismutation) and decrease with the reduction in total acidity. The activity of the samples in the total conversion of toluene increseas in the following order: Sample C < Sample B < Sample A.

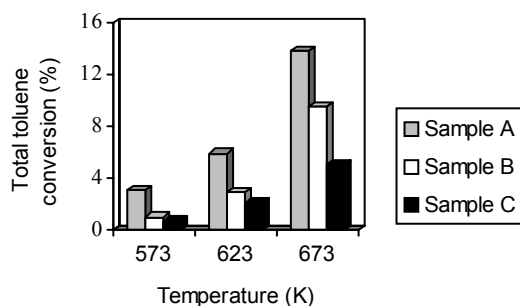


Figure 7. Influence of the reaction temperature and isomorphous substitution degree on the total conversion of toluene

The disproportionation reaction is accompanied by secondary reactions like dealkylation reaction. The total conversion of toluene is the sum between the intrinsic dismutation and dealkylation reactions. For example, at 573 K (low conversion levels) the competition between these reactions is illustrated in Figure 8a. It is shown that the sample A (most acide) is the most active in disproportionation reaction, while the sample C presented low activity, but for all the samples the disproportionation of toluene was predominant. The results can be explained in acidity terms and according to the concentrations of acid sites (Table 3). A decrease in catalytic activity is observed when the amount of framework gallium is decreased.

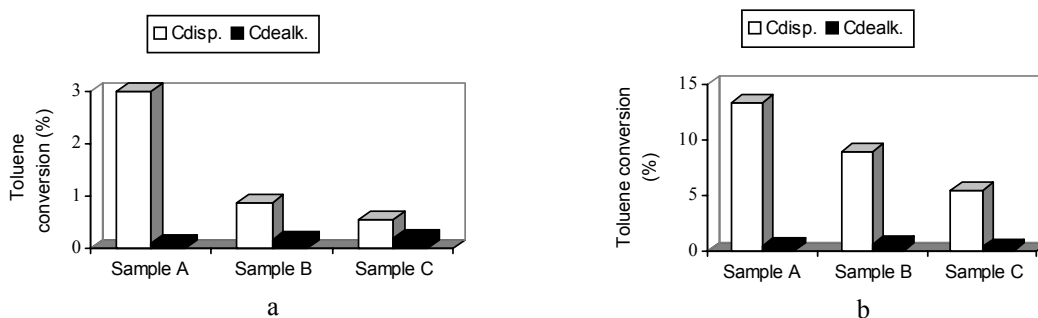


Figure 8. The influence of the isomorphous substitution degree on the conversion of toluene into disproportionation and dealkylation reactions at 573 K (a) and 673 K (b)

The same behavior is observed at 673 K (high values of toluene conversion) (Figure 8b) which shows that the importane of the secondary reactions is very weak, whereas, the disproportionation of toluene clearly takes place.

With regard to the conversion of toluene into xylenes, the highest values of xylenes are also obtained on the most acid sample of (Si,Ga)-MCM-22 (sample A) for the three studied temperatures (Figure 9). The conversion rate of toluene in xylenes increases with the increase of the temperature and is diminished with the isomorphous degree of substitution.

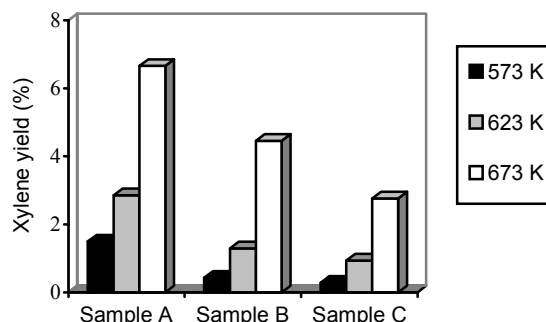


Figure 9. The influence of the reaction temperature and isomorphous substitution degree on the conversion of toluene into xylenes

In the range of the temperature studied (573 – 673 K), the disproportionation of toluene generated mixed xylenes, but for all the temperatures the fraction of *p*-xylene is greater than the thermodynamic equilibrium value (~ 24 %) on the sample A (Figure 10). The fraction of *m*- and *o*-xylenes increased with the temperature, while the *p*-xylene decreased, but it was always predominantly. This selectivity for *p*-xylene can be explained by the difference in diffusivity of xylene isomers. The disproportionation of toluene involves a bulky intermediate [4, 10] and on the MCM-22 zeolite the reaction take place on the external surface in 12-MR. *p*-Xylene which is the primary product among the xylenes isomers (diameter 0.67 nm) presented fast diffusion into 10-MR channels of MCM-22, compared to *m*- (0.71 nm) and *o*-xylenes (0.74 nm). The fast diffusion of *p*-xylene and the restricted diffusion of *o*-xylene have been reported on MCM-22 zeolite [46, 47]. For the high temperatures, the diminished fraction of *p*-xylene can be due to the further isomerisation of *p*- to *m*- and *o*-xylene. However, for all the temperatures studied, these isomers can be arranged on the order: *para*- > *meta*- > *ortho*-xylenes.

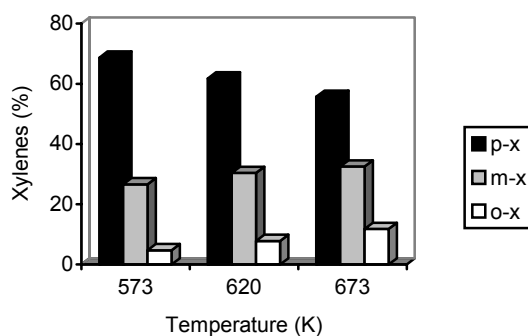


Figure 10. The influence of the reaction temperature on the xylene concentration over sample A of (Si,Ga)-MCM-22 zeolite

The *p*-xylene proportion is further enhanced by isomorphous substitution degree. The distribution of *p*-xylene for the three samples of (Si,Ga)-MCM-22 is presented in Figure 11 as a function of the temperature reaction.

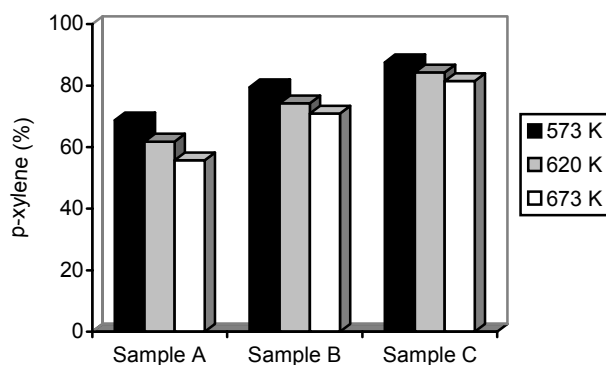


Figure 11. The influence of the isomorphous degree and the temperature reaction on the fraction of *p*-xylene for the three sample of (Si,Ga)-MCM-22 zeolite

For sample A, at the low temperature, 573 K (conversion level of toluene, ~3 %), the fraction in *p*-xylene was 68.7 % and increased at 87.6 % for the sample C, when isomorphous substitution degree increased. At high temperatures, 673 K (conversion of toluene ~ 14 %), the fraction in *p*-xylene for the sample A decreased at 55.7 % and for the sample C at 81.5 %. The *p*-xylene proportion is very high for the sample C which presented low acidity. The enhancement of the *p*-xylene for all the samples, but specially for the sample C was due to the isomorphous substitution phenomenon which determined the decrease in the number and the force of the acid sites, especially on the external surface (in the supercages). In addition, if we compare the fraction in *p*-xylene obtained on the (Si,Al)-MCM-22 zeolite [48 – 50], with those of the (Si,Ga)-MCM-22 zeolite, we can be conclude that the acidity spectrum plays an important role. It is well known that the gallosilicates show a reduced acidity compared to the aluminosilicates. The isomorphous substitution of the (Si,Ga)-MCM-22 zeolite, enhances the *p*-selectivity, mainly by suppressing further the isomerization of the primary product in toluene disproportionation (*p*-xylene) to *m*-xylene on the strongest acid sites. The results are in agreement with those reported by Wu et.al [12] on the dealuminated (Si,Al)-MCM-22 zeolite where the high *p*-selectivity is explained in terms of the acidity of the samples.

CONCLUSIONS

Three samples of (Si,Ga)-MCM-22 zeolite with Si/Ga ratios of 18, 71 and 89 have been synthesized hydrothermally under static conditions, but the pure phase of zeolite was obtained only for Si/Ga = 18. The presence of Ga in the tetrahedral framework position is evidenced by a variety of techniques. The acidic properties have been studied by TPD of ammonia, showing that the acid character depends on the gallium concentration. The catalytic performances of (Si,Ga)-MCM-22 zeolite with various Ga contents have been

studied in the toluene disproportionation reaction in the temperature range 573 – 673 K. The fraction of *p*-xylene increased with the isomorphous substitution degree and decreases with the temperature. The high *para*-selectivity observed, can be attributed to a combination of intrinsic structure, the different diffusivity rate of the xylene isomers and the acidity of the samples. By using the samples with reduced acidity, the undesired reactions can be minimized in order to enhance the disproportionation reaction to xylenes, especially to *p*-xylene.

REFERENCES

1. Tsai, T.C., Liu, S.-B., Wang, I.: *Appl. Catal. A*, **1999**, **181**, 355;
2. Sherman, J.D.: *Proc. Natl. Acad. Sci. USA*, **1999**, **96**, 3471;
3. Haag, W.O., Olson, D.H., Rodewald, P.G.: *U.S. Patent 4,358,395*, **1982**;
4. Kaeding, W.W., Chu, C., Young, L.B., Butter, S.A.: *J. Catal.*, **1981**, **69**, 392;
5. Olson, D.H., Haag, W.O.: *ACS Symp. Ser.* **1984**, **248**, 275;
6. Meshram, N.R., Hegde, S.G., Kulkarni, S.B., Ratnasamy, P.: *Appl. Catal. A*, **1983**, **8**, 359;
7. Uguina, M.A., Sotelo, J.L., Serrano, D.P., Valverde, J.L.: *Ind. Eng. Chem. Res.* **1994**, **33**, 26;
8. Wang, I., Tsai, T.Ch., Huang, Sh.T.: *Ind. Eng. Chem. Res.*, **1990**, **29**, 2005;
9. Das, J., Bhat, Y.S., Halgeri, A.B.: *Catal. Lett.*, **1994**, **23**, 161;
10. Xiong, Y.S., Rodewald, P.G., Chang, C.D.: *J. Am. Chem. Soc.*, **1995**, **117**, 9427;
11. Juttu, G.G., Lobo, R.F.: *Micropor. Mesopor. Mater.*, **2000**, **40**, 9;
12. Wu, P., Komatsu, T., Yashima, T.: *Micropor. Mesopor. Mater.*, **1998**, **22**, 343;
13. Mavrodinova, V., Popova, M.: *Catal. Commun.*, **2005**, **6**, 247;
14. Rubin, M.K., Chu, P.: *US Patent 4,954,325*, **1990**;
15. Leonowicz, M.E., Lawton, J.A., Lawton, S.L., Rubin, M.K.: *Science*, **1994**, **264**, 1910;
16. Millini, R., Perego, G., Parker Jr., W.O., Bellussi, G., Carluccio, L.: *Micropor. Mater.*, **1995**, **4**, 221;
17. Lawton S.L., Leonowicz M.E., Partridge R.D., Chen P., Rubin M.K.: *Micropor. Mesopor. Mater.*, **1998**, **23**, 109;
18. Baerlocher, Ch., Meier, W.M., Olson, D.H.: *Atlas of Zeolite Framework Types*, 5th ed., Elsevier, Amsterdam **2001**;
19. Zhu, Z., Chen, Q., Xie, Z., Yang, W., Li, C.: *Micropor. Mesopor. Mater.*, **2006**, **88**, 16;
20. Souverijns, W., Verrelst, W., Vanbutsele, G., Martens, J.A., Jacobs, P.A.: *Chem. Commun.*, **1994**, 1671;
21. Unverricht, S., Hunger, M., Ernst, A., Karge, H.G., Weitkamp, J.: *Studies in Surface Science and Catalysis*, vol 84, (Editors: Weitkamp, J., Karge, H.G., Pfeifer, H., Holderich, W.), Elsevier, Amsterdam, **1994**, **84**, 37;
22. Chu, C.T., Chang, C.D.: *J. Phys. Chem.*, **1985**, **89**, 1569;
23. Kumar, N., Lindfors, L.E.: *Appl. Catal. A* **1996**, **147**, 175;
24. Corma, A., Corell, C., Pérez-Pariente, J.: *Zeolites*, **1995**, **15**, 2;
25. Guray, I., Warzywoda, J., Bac, N., Sacco Jr., A.: *Micropor. Mesopor. Mater.*, **1999**, **31**, 241;

26. Lawton, S.L., Fung, A.S., Kenedy, G.J., Alemany, L.R., Chang, C.D., Hatzikos, G.H., Lissy, D.N., Rubin, M.K., Timken, C., Steuernagel, S., Woessner, D.E.: *J.Phys. Chem.*, **1996**, **100**, 3788;
27. Cambor, M.A., Corma, A., Diaz-Cabanas, M.J.: *J. Phys. Chem. B*, **1998**, **102**, 44;
28. Ravishankar, R., Bhattacharya, D., Jacob, N.R., Sivasanker, S.: *Microporous Mater.*, **1995**, **4**, 83;
29. Okumura, K., Hashimoto, M., Mimura, T., Niwa, M.: *J.of Catalysis*, **2002**, **206**, 23;
30. Corma, A., Soria, V.M., Schnoefeld, E.: *J. of Catalysis*, **2000**, **192**, 163;
31. Dahlhoff, G., Barsnick, U., Holderich, W.F.: *Appl. Catal. A*, **2001**, **210**, 83;
32. Corma, A., Corell, C., Fornés, V., Kolodziejski, W., Pérez-Pariente, J.: *Zeolites*, **1995**, **15**, 576 ;
33. Hazm, J.E., Caullet, P., Paillaud, J.L., Soulard, M., Delmotte, L.: *Micropor. Mesopor. Mater.*, **2001**, **43**, 11;
34. Occelli, M.L., Eckert, H., Wolker, A., Auroux, A.: *Micropor. Mesopor. Mater.*, **1999**, **30**, 219;
35. Occelli, M.L., Schweizer, A.E., Fild, C., Schwering, G., Auroux, A.: *J. of Catalysis*, **2000**, **192**, 119;
36. Wolker, A., Hudalla, C., Eckert, H., Auroux, A., Occelli, M.L.: *Solid State Nuclear Magnetic Resonance*, **1997**, **9**, 143;
37. Hunger, M., Ernst, S., Weitkamp, J.: *Zeolites*, **1995**, **15**, 188;
38. Kennedy, G.D., Lawton, S.L., Rubin, M.K.: *J. Am. Chem. Soc.*, **1994**, **116**, 11000;
39. Cambor, M.A., Corell, C., Corma, A., Diaz-Cabanas, M.-J., Nicolopoulos, S., Gonzalez-Calbet, J.M., Vallet-Regi, M.: *Chem. Mater.*, **1996**, **8**, 2415;
40. Kolodziejski, W., Zicovich-Wilson, C, Corell, C., Perez-Pariente, J., Corma, A.: *J.Phys. Chem.*, **1995**, **99**, 7002;
41. He, H.J., Nivarthi, G.S., Eder, F., Seshan, K., Lercher, J.A.: *Micropor. Mesopor. Mater.*, **1998**, **25**, 207;
42. Chen, N.Y., Garwood, W.E., Dwyer, F.G.: *Shape Selective Catalysis in Industrial Applications*, Marcel Dekker, New York, **1989**;
43. Borade, R.B.: *Zeolites*, **1987**, **7**, 398;
44. Axon, S.A., Huddersman, K., Klinowski, J.: *Chem. Phys. Lett.*, **1990**, **172**, 398;
45. Szostak, R., Thomas, T.L.: *J. Catal.*, **1986**, **100**, 555;
46. Roque-Malherbe, R., Wendelbo, R., Mifsud, A., Corma, A.: *J. Phys. Chem., B* **1995**, **99**, 14064;
47. Wendelbo, R., Roque-Malherbe, R.: *Micropor.Mater.* **1997**, **10**, 231;
48. Corma, A., Corell, C., Perez-Pariente, J., Guil, J.M., Guil-Lopez, R., Nicolopoulos, S., Calbet, J.G., Vallet-Regi, M.: *Zeolites*, **1996**, **16**, 7;
49. Weitkamp, J., Weiss, U., Ernst, S.: *Studies of Surface Science and Catalysis* (Editors: Beyer, H.K., Karge, H.G., Kiricsi, I., Nagy, J.B.), Elsevier, Amsterdam, **1995**;
50. Corma, A., Corell, C., Llopis, F., Martinez, A., Perez-Pariente, J.: *Appl. Catal., A* **1994**, **115**, 121.